TECTONICS, VOL. 19, NO. 1, PAGES 153-167 FEBRUARY 2000

The late exhumation history of the ultrahigh-pressure Maksyutov Complex, south Ural Mountains, from new apatite fission track data

Mary L. Leech[1] and Daniel F. Stockli[2]

Geological and Environmental Sciences, Stanford University, Stanford, California

Abstract. Apatite fission track samples were collected from the ultrahigh-pressure (UHP) Maksyutov Complex, south Ural Mountains, in the footwall of the Main Uralian fault (MUF) to constrain the low-temperature cooling history and to establish the late stage exhumation rate for the complex. Fission track samples were taken along a 70-km north-south transect and a 5-km east-west traverse through the Maksyutov Complex, with two samples from the hanging wall of the MUF. Apparent age and track length modeling results indicate that the Maksyutov Complex was exhumed and cooled to 110°C en masse in the Early Permian (300 ± 25 Ma). The east-west transect shows that no significant interunit movement occurred in the Maksyutov Complex after ~315 Ma; on the basis of higher-temperature thermochronometers, the entire Maksyutov Complex must have been assembled between 335 and 315 Ma. Modeling for the north-south transect indicates that exhumation occurred contemporaneously in the north and south regions of the complex with cooling to 110°C between 375 and 315 Ma, coinciding with the onset of the Uralian orogeny. Comparison of modeling for Maksyutov samples and an Ordovician metasediment from the hanging wall of the MUF indicates that late movement on the MUF was minor and that the footwall and hanging wall had a similar cooling history after the late Carboniferous (~300 Ma). Exhumation rates range from 0.3 to 1.5 mm yr^{-1} between a high-pressure metamorphic event at 375 and 315 Ma using current heat flow data. Our calculated exhumation rate for the Maksyutov Complex is consistent with the complex being a UHP terrane, even though coesite and diamond are not preserved.

1. Introduction

The Ural Mountains, with a modern crustal thickness of up to 55 km (based on the Urals Reflection Seismic Experiment and Integrated Studies (URSEIS) seismic reflection-refraction profile shown in Figure 1) and topography of no more than 1600 m in the south, differ from other Paleozoic orogens (e.g., the Variscides, Caledonides, and Appalachians) by preserving a collisional structure that lacks large-scale late orogenic extension [*Dewey*, 1988; *Berzin et al.*, 1996; *Echtler and Hetzel,* 1997; *Knapp et al.*, 1998]. One method to constrain the extension history may be to investigate the late stage evolution of the most important suture zone in the Urals, the Main Uralian fault (MUF).

The ultrahigh-pressure (UHP) Maksyutov Complex forms the footwall to the MUF in the south Urals and records a petrologic history since the onset of collision in the south Urals. Current thermochronological data for this complex constrain a high-pressure (HP) stage of its history and cooling through 350°C [e.g., *Beane*, 1997; *Shatsky et al.*, 1997] but provide little information about the assembly of the complex, its final exhumation along the MUF zone, and the geomorphic evolution of the southern part of the mountain belt. Apatite fission track (AFT) thermochronology is an effective tool for reconstructing cooling histories, recording information on the timing and rate of late stage exhumation.

In this paper, AFT data describe the low-temperature cooling history for the Maksyutov Complex and regionally for the south Ural Mountains. In particular, the collection of AFT ages and confined track length data in conjunction with thermal modeling is a powerful means to obtain a more comprehensive picture of the multistage thermal evolution of the rocks currently exposed in the south Ural Mountains, to fill gaps in the history of the Maksyutov Complex that recent workers [i.e., *Beane et al.*, 1995; *Lennykh et al.*, 1995; *Dobretsov et al.*, 1996; *Hetzel et al.*, 1998] have been unable to fully address, and to constrain the timing and magnitude of movement on the MUF. Furthermore, these data also help us to better understand the crustal mechanics of how ultrahigh-pressure rocks are exhumed to the surface.

Reports of coesite and coesite pseudomorphs [*Chesnokov and Popov*, 1965; *Dobretsov and Dobretsova*, 1988] and graphite pseudomorphs after diamond [*Leech and Ernst*, 1998] from the Maksyutov Complex suggest that these rocks have been metamorphosed at ultrahigh pressures. The processes by which buoyant continental crust is subducted to depths exceeding 100 km and later returned to the surface are not yet well known, but a necessary and often lacking piece of information is the complete pressure-temperature-time path. In particular, the exhumation rate may set important constraints on the mechanism for exhumation. It is clear from this work that extension on the MUF did not play a major role in the late exhumation of Maksyutov eclogites after ~300 Ma and that the exhumation rate was slow, failing to preserve coesite or diamond. Although UHP metamorphism is only described in a few terranes, it is quite probable that its preservation is limited mainly by the exhumation process;

[1]Also at Geology Department, Royal Holloway University of London, Egham, England, United Kingdom.
[2]Now at Geological and Planetary Sciences, California Institute of Technology, Pasadena.

Paper number 1999TC900053.
0278-7407/00/1999TC900053$12.00

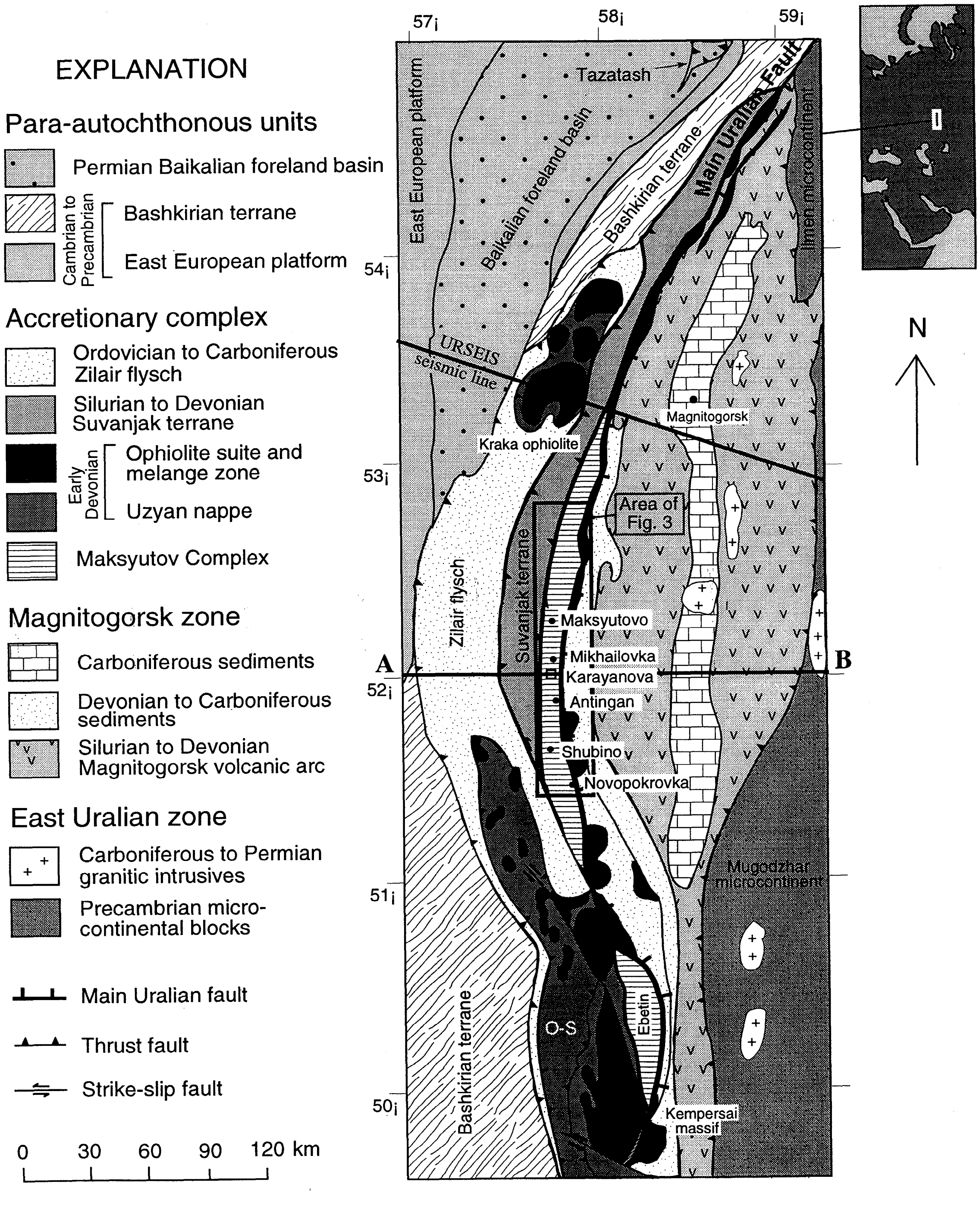

Figure 1. Tectonostratigraphic map of the south Ural Mountains [after *Beane et al.*, 1995] showing the areas where apatite fission track (AFT) samples were collected and the location of Figure 3. The 1995 the Urals Reflection Seismic Experiment and Integrated Studies (URSEIS) seismic line is shown north of the Maksyutov Complex. Cross section A-B is shown in Figure 2.

perhaps other high-grade terranes worldwide have experienced UHP metamorphism, but exhumation rates were too low to preserve indicator minerals.

2. Tectonic Setting of the South Ural Mountains

The Urals are a 2000-km-long, 400 to 450 km-wide orogen formed by oblique collision between the East European platform and microcontinental blocks to the east in Late Devonian to Permian time [*Zonenshain et al.*, 1984, 1990; *Coleman et al.*, 1993]. Figure 1 is a tectonostratigraphic map of the south Urals showing the relative position of the Maksyutov Complex within the orogen. The south Ural Mountains are divided into four main tectonic units; from west to east they are the following: para-autochthonous units that include the East European platform, the foreland basin, and the fold-and-thrust belt; an accretionary complex including the shelf and slope sediments of the Zilair and Suvanjak terranes, ophiolitic thrust sheets, and the Maksyutov Complex; the Magnitogorsk zone which contains a volcanic arc with Devonian to Carboniferous sediments; and the East Uralian zone composed of microcontinental blocks and late granitic intrusions.

The East European platform is overlain on the east by the Upper Ordovician to lower Carboniferous Zilair nappe (also known as the Sakmara) clastic wedge sediments. The Zilair nappe is thrust westward over the strongly deformed Silurian - Lower to Middle Devonian slope-derived sediments and volcaniclastics of the Suvanjak terrane [*Brown et al.*, 1996], forming the western boundary to the Maksyutov Complex (Figure 1).

Part of the leading edge of the East European platform was subducted beneath the Magnitogorsk island arc complex supplying the sedimentary protolith to the Maksyutov Complex. An early phase of extension, preserved as a series of deep, extensional basins beneath the Uralian foreland, along the eastern margin of the East European platform, likely resulted in the shallow intrusion of mafic sills or dikes within the sedimentary section [*Puchkov*, 1997; *Diaconescu et al.*, 1998; *Brown and Spadea*, 1999]; these mafic intrusions probably constitute the basaltic protolith for eclogite in the Maksyutov Complex. *Edwards and Wasserburg* [1985] report Sm-Nd wholerock dates for the Kempersai ophiolite (Figure 1) in the southernmost Urals of 397 ± 20 Ma, and they interpret this as the igneous crystallization age for pre-Uralian oceanic crust. These ophiolites may be related to the ophiolites in the hanging wall of the MUF and are represented by the Kraka ophiolite, a remnant klippe of the early westward directed thrusting on the MUF [*Matte et al.*, 1993; *Savelieva et al.*, 1997]. Figure 2 shows the current cross-sectional relationship between the Maksyutov Complex and the other tectonic units shown in Figure 1 and a cartoon showing the same units in the Early to Middle Devonian.

The MUF is the main suture zone of the Urals and extends over 2000 km along its axis (Figure 1); in the south Urals it is a diffuse mélange zone (up to 20 km wide) containing ophiolitic rocks and Lower to Middle Devonian blocks derived from the Magnitogorsk arc to the east, all in a serpentinite matrix [*Puchkov*, 1993; *Zakharov and Puchkov*, 1994; *Brown et al.*, 1996]. The youngest rocks involved in faulting along the MUF are lower Carboniferous in the southernmost areas; in the central northern Urals the MUF is overlain by Jurassic to Lower Cretaceous sediments [*Brown et al.*, 1996].

The Magnitogorsk island arc complex contains Upper Silurian to Upper Devonian volcanic and volcaniclastic rocks with overlying Carboniferous interarc basin sediments [*Zonenshain et al.*, 1984; *Brown et al.*, 1996]. The ophiolites and island arc assemblages are folded into an open syncline and overprinted by low-grade metamorphism. The Magnitogorsk island arc complex was thrust eastward over the Vendian to Ordovician Mugodzhar and Ilmen microcontinents [*Zonenshain et al.*, 1990].

The Mugodzhar microcontinent (Figure 1), now composed of migmatites and granulites, probably rifted from continental blocks to the east of the orogen (i.e., the Siberian or Kazakhstan cratonal blocks) during the Early Ordovician [*Puchkov*, 1997; *Savelieva et al.*, 1997]. Late Carboniferous to Permian granitic plutons intrude the island arc complex and microcontinents and may be related to eastward subduction of continental crust beneath the Magnitogorsk island arc complex [*Zonenshain et al.*, 1990].

3. Geologic Background of the Maksyutov Complex

The Maksyutov Complex trends north-south and consists of three main units tectonically juxtaposed within the same subduction zone: an eclogite-bearing gneiss, called Unit 1; a blueschist facies Yumaguzinskaya metasedimentary unit lacking eclogite; and a meta-ophiolite mélange, termed Unit 2 (Figure 2). Unit 1 contains boudins of eclogite, layers of eclogitic gneiss, and rare ultramafic bodies within host metasedimentary mica schist and quartzite. The sedimentary protolith to Unit 1 host rocks was part of the leading edge of the subducting East European platform; the eclogite bodies were most likely derived from mafic intrusions associated with an early extensional event in the foreland. The Yumaguzinskaya contains protolith rock types similar to those of Unit 1 but is metamorphosed to no more than lower blueschist facies or upper greenschist facies based on metamorphic mineral assemblages, representing a lesser depth of subduction than that of the UHP Unit 1 rocks. Unit 2, with an oceanic crust affinity, consists of lenses of serpentinite mélange and blocks of metasomatic rock (approximately rodingite), metabasalt, and Ordovician to Silurian marble within mica schist and graphite quartzite host rock [*Dobretsov et al.*, 1996]; peak metamorphism for Unit 2 was blueschist to upper greenschist facies.

Unit 2 and the Yumaguzinskaya, considered to tectonically overlie Unit 1 [*Lennykh et al.*, 1995], were juxtaposed with Unit 1 most likely in the subduction zone after the Early to Middle Devonian UHP metamorphic event that affected Unit 1 (*Matte et al.* [1993], *Beane et al.* [1995], *Beane* [1997], and this study). All three units were overprinted by a late, low-pressure, greenschist facies metamorphism and subsequently folded together about NE-SW trending axes (Figure 2).

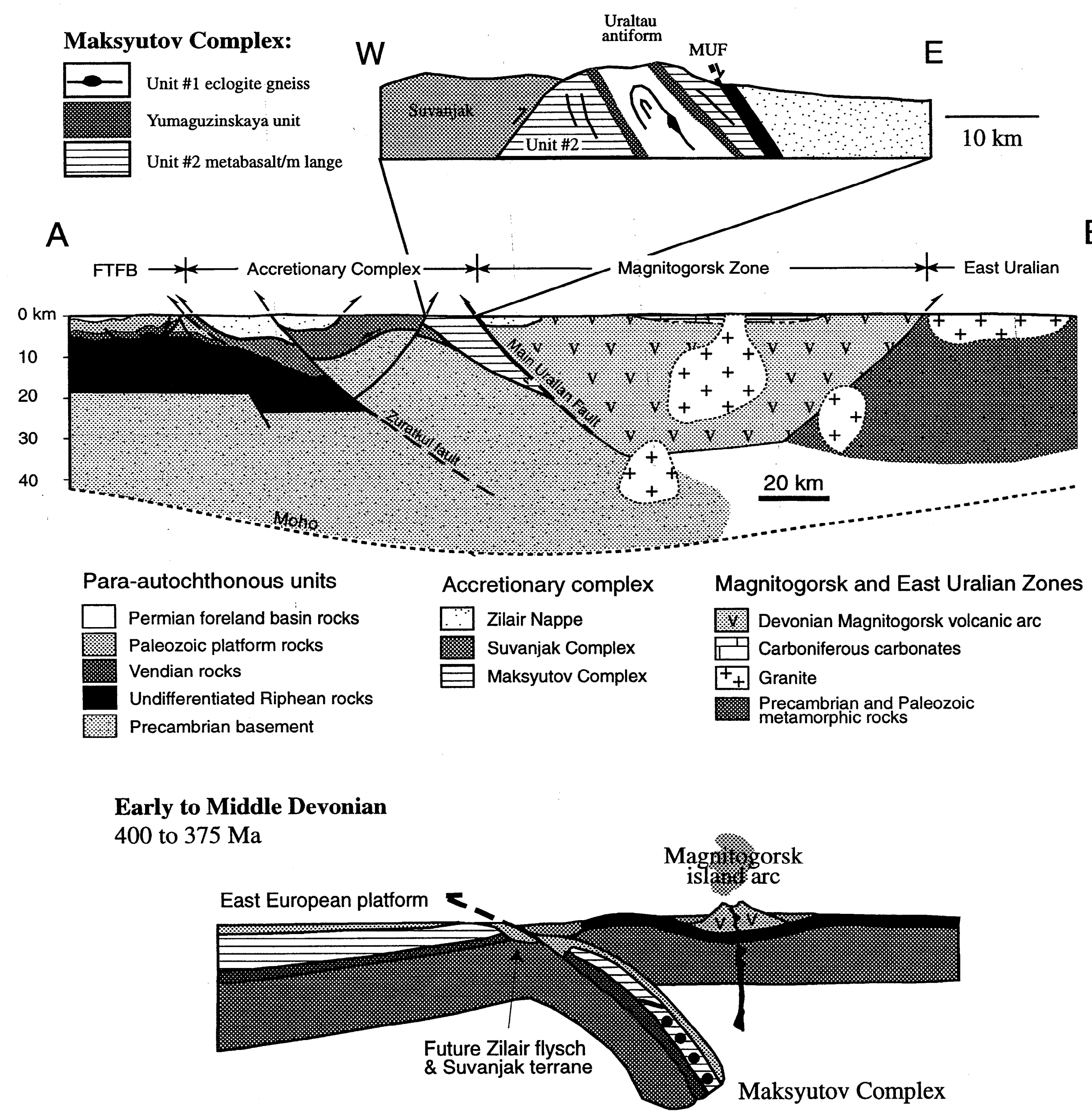

Figure 2. Schematic upper crustal cross section A - B (from Figure 1) across the south Urals through Karayanova showing the structural relationships from the foreland basin in the west to the East Uralian zone (adapted from *Brown et al.* [1998]). An expanded cross section through the Karayanova area shows the large-scale relationship between the units. Cartoon at the bottom shows the relative position of the tectonic units in the Early to Middle Devonian. No vertical exaggeration is shown. MUF, Main Uralian fault; FTFB, foreland fold-and-thrust belt.

Fe-Mg exchange geothermometry calculated for garnet and clinopyroxene from eclogite yields an equilibrium temperature ranging from 594° to 637°C [*Powell*, 1985]. Minimum pressure estimates using the jadeite component of clinopyroxene [*Holland*, 1980] range from 1.5 to 1.7 GPa (*Beane et al.* [1995], *Lennykh et al.* [1995], and this study) and may be as high as 2.7 GPa [*Bohlen and Boettcher*, 1982] if coesite pseudomorphs described in eclogite from *Shubino* [*Chesnokov and Popov*, 1965] and jadeite quartzite from Karayanova [*Dobretsov and Dobretsova*, 1988] are interpreted correctly. In addition, graphite phengite schist from near the former village of Karayanova contains unusual cuboid graphite aggregates that deflect a foliation defined by phengite and elongate graphite grains. These graphite aggregates may be pseudomorphs after diamond, which would indicate UHP [*Leech and Ernst*, 1998]. Thermobarometric estimates may represent annealing during exhumation in which minerals reequilibrated at lower pressure-temperature (*P-T*) conditions, leaving little evidence of UHP metamorphism.

4. Interpretation of Previous Age Dating for the UHP Metamorphic Event

Matte et al. [1993] reported a 380 Ma $^{40}Ar/^{39}Ar$ age from eclogitic white mica and argued that a rapid exhumation rate did not allow phengites to reequilibrate after the UHP event and thus the 380 Ma represents the age of UHP metamorphism. These data are corroborated by similar $^{40}Ar/^{39}Ar$ ages from *Beane* [1997] that range from 372 ± 3 to 377 ± 3 Ma for phengite from eclogite in Unit 1. However, Beane interpreted these data as a cooling age during exhumation, assuming a closure temperature (T_c) for white mica of ~350° ± 50°*C* [*Purdy and Jager*, 1976], because thermobarometry for Maksyutov indicates a minimum metamorphic temperature of 594° - 637°*C* [*Leech and Ernst*, 1998]. Unit 2 $^{40}Ar/^{39}Ar$ ages indicate cooling from 339 ± 3 to 332 ± 3 Ma; ages from the Yumaguzinskaya unit range from 356 ± 3 to 365 ± 2 Ma [*Beane*, 1997]. The difference in ages for Unit 1, the Yumaguzinskaya, and Unit 2 represents the times the units cooled through 350°C during exhumation. When these cooling ages are viewed in conjunction with AFT data from this study, it is clear that the three units were juxtaposed between ~335 and 315 Ma.

Preliminary $^{206}Pb/^{238}U$ analyses on rutile from eclogite in Unit 1 give concordant ages of ~377 ± 2 Ma from Shubino and 384 ± 4 Ma from Karayanova, which is interpreted as the age of the UHP event [*Beane et al.*, 1996; *Beane et al.*, 1997]. These ages are similar to the 372 ± 3 to 377 ± 3 Ma $^{40}Ar/^{39}Ar$ dates; the closeness of these ages is interpreted as indicating a rapid exhumation [*Beane*, 1997]. However, the closure temperature for U-Pb in rutile is not well constrained. *Zalduegui et al.* [1996] reports a T_c for rutile of ~650°C based on similar U-Pb ages from coexisting minerals such as zircon, monazite, and titanite. *Mezger et al.* [1989] describes the dependency of the T_c on composition, cooling rate, grain size, and the geometry for each phase analyzed before the ages can be interpreted correctly. Mezger et al. suggests a T_c for U-Pb in rutile of ~420°C for a cooling rate from 0.5° to 1°C Myr^{-1} and a grain radius from 0.009 to 0.021 cm and a T_c of 380°C for a grain radius from 0.007 to 0.009 cm.

The T_c for U-Pb in rutile and $^{40}Ar/^{39}Ar$ in phengite overlap within their error limits; their respective ages probably reflect the same event, a cooling age rather than the age of the UHP event. The ages obtained thus far by $^{40}Ar/^{39}Ar$ and U-Pb techniques represent cooling through 380° to 350°C, much lower than the 600°C temperature calculated from thermobarometry, and these ages apparently do not represent the age of the highest-pressure metamorphic event.

Shatsky et al. [1997] report Sm-Nd ages ranging from 357 ± 15 to 378 ± 13 Ma that suggest an event at ~375 ± 3 Ma. The closure temperature in garnets for the Sm-Nd system is ~600 ± 30°*C* for garnets with a diameter between 0.1 and 5 cm [*Mezger et al.*, 1992]. These Sm-Nd data overlap considerably with lower-temperature systems, unlike an unpublished Sm-Nd date of 404 ± 20 Ma (R.J. Beane, personal communication, 1998). The presumption that these data give the age of UHP metamorphism [*Shatsky et al.*, 1997; *Hetzel et al.*, 1998] is premature. Additional high-temperature thermochronology in a well-known chemical system (i.e., U-Pb in zircon) is necessary before we can set additional age constraints on the UHP metamorphic event for Maksyutov; at the same time, sensitive high-resolution ion microprobe (SHRIMP) dating of the cores of these zircons may also provide limits on the Precambrian sedimentary protolith to Unit 1 rocks.

5. Apatite Fission Track Dating for the Maksyutov Complex

5.1. Fission Track Thermochronology

Fission tracks are linear damage trails that form in the crystal lattice as the result of spontaneous nuclear fission of trace ^{238}U in minerals such as apatite and zircon [e.g., *Fleischer et al.*, 1975]. Spontaneous fission occurs at an essentially constant rate, so the number of tracks may be used to calculate fission track ages. In early studies, fission track ages were commonly interpreted simply as cooling ages, dating when a sample cooled through a mineral-specific closure temperature [*Dodson*, 1973] during exhumation (e.g., 110°C for apatite).

In recent years this technique has been augmented by more sophisticated approaches that use apparent age, single-grain age, and confined track length data to interpret the thermotectonic history with modeling techniques. The use of these data for thermochronology relies on the fact that tracks are partially or entirely erased by thermally induced recrystallization at elevated temperatures. This process, referred to as annealing, causes easily measured reductions in both track lengths and fission track ages [e.g., *Naeser*, 1979, 1981; *Gleadow et al.*, 1986a, b; *Green et al.*, 1989a, b; *Crowley et al.*, 1991; *Corrigan*, 1991, 1992; *Tagami et al.*, 1998]. At geologic cooling rates, significant track length and apparent age reduction occurs between ~60° and 110°C, termed the Partial Annealing Zone (PAZ). All apatite fission tracks are completely erased at temperatures greater than ~110° - 135°C, depending in part on apatite composition and the timescale of geologic heating [e.g., *Corrigan*, 1992]. At shallow levels above the PAZ, track length shortening is minimal owing to low ambient temperatures; ages are older and date earlier thermal events or retain detrital provenance ages, depending on the particular circumstances.

Apatite fission track data from rocks that underwent rapid exhumation from structural levels below the PAZ to near-surface levels are characterized by ages that are essentially invariant; track length distributions are unimodal, narrow, and have long mean lengths [*Gleadow et al.*, 1986b; *Green et al.*, 1989b; *Fitzgerald and Gleadow*, 1990]. However, in the case of slow, protracted cooling and exhumation or later reheating within the PAZ, track lengths are characterized by either bimodal or negatively skewed unimodal distributions with mean track lengths that are significantly shorter than those in the case of rapid exhumation [*Gleadow et al.*, 1986b; *Green et al.*, 1989b]. Samples that underwent slow cooling, residing within the PAZ at elevated temperatures for geologic time, will yield partially annealed, apparent AFT ages that do not directly date cooling and are usually unrelated to a specific thermal or tectonic event. Modeling methods incorporating age and track length data can interpret partially annealed data and decipher the thermal histories undergone by such samples.

5.2. Sample Preparation and Laboratory Methods

Apatites were separated using standard mineral separation techniques [e.g., *Dumitru*, 2000]; apatite yields were low because of the small sample size (< 0.5 - 1.0 kg) but sufficient for dating. While hanging wall sample MC144-95 (Novopokrovka) has a uranium concentration of 19 ppm, uranium concentrations in Maksyutov Complex apatites are low, most ranging from ~3 to 9 ppm U. MK-115 had a small number of induced tracks owing to very low uranium content (~0.5 ppm) giving an age of 311 ± 45 Ma, which is statistically not significantly different at the 2σ level from the rest of the age population, clustering at ~256 Ma (Table 1).

All apatites were etched for 20 seconds in 5 N nitric acid at room temperature. Grains were dated by the external detector method with muscovite detectors. The CN5 dosimetry glass was used as a neutron flux monitor. Samples were irradiated in well-thermalized positions at the Oregon State University reactor. External detectors were etched in 48% HF. Tracks were counted with Zeiss Axioskop microscope with x100 air objective, x1.25 tube factor, x10 eyepieces, and transmitted light with supplementary reflected light as needed; external detector prints were located with a Kinetek automated scanning stage [*Dumitru*, 1993]. Confined, horizontal track lengths were measured only in grains with *c*- axes subparallel to slide plane (within ±5°-10°), following protocols of *Laslett et al.* [1982]. Lengths were measured with a computer digitizing tablet and drawing tube, calibrated against the stage micrometer [e.g., *Dumitru*, 1993].

5.3. Fission Track Results and Discussion

Fifteen AFT samples were analyzed from north-south and east-west transects across the Maksyutov Complex and from Ordovician metasediments in the hanging wall of the MUF to constrain the low-temperature cooling history (Table 1). Apparent ages for all samples from the Maksyutov Complex range from 210.4 ± 12.5 to 311.5 ± 45.4 Ma, whereas two samples from the hanging wall of the MUF are 198.4 ± 15.3 and 279.2 ± 36.3 Ma.

Figure 3 shows apparent ages and confined track length distributions for 12 samples (most with confined track length data $n > 80$; hanging wall sample MC-143-95 has 57 measured track lengths and is included for comparison purposes). Twelve Maksyutov samples intersect the weighted mean age of 256 ± 7 Ma within 1σ. Confined track length data have unimodal distributions with mean track lengths ranging from 12.25 to 13.99 μm, suggesting that all samples underwent partial annealing. Track length distributions often show a tail of shorter tracks, indicating some annealing of early formed tracks while residing in the PAZ at elevated temperatures (100° - 80°*C*). Figure 4 shows a plot of apparent AFT ages versus mean track lengths for footwall and hanging wall samples within the Maksyutov Complex; all samples fall within a fairly small region of ages and mean track lengths.

6. Fission Track Modeling

The apparent, partially annealed AFT ages and the confined track length data were used to reconstruct the low-temperature (T < 110°C) evolution of the UHP Maksyutov Complex. Track length distributions for all samples with sufficient numbers of confined tracks (n > 80, except for MC-143-95] were modeled using the modeling program of *Gallagher* [1995], "Monte Trax," employing a Monte Carlo type approach with a genetic algorithm; this stochastic modeling allows us to input fission track (FT) data and to specify upper and lower limits for both time and temperature during model runs, and it uses an assumed initial track length of 16.3 μm. The temperature-time (T-t) boundary conditions for model runs were set freely using additional independent geologic data, such as higher-temperature $^{40}Ar/^{39}Ar$ thermochronologic data from Unit 1, age of deposition, and present-day surface temperature, allowing the model maximum freedom within those bounds. The modeling program, using experimentally derived annealing data by *Laslett et al.* [1987], chooses points at random within these bounds which then become the nodes for linear segments adopted for the first-run thermal history. Model data obtained from this initial run are compared to the observed FT data; with each succeeding iteration the model run data try to improve the fit between predicted and observed AFT data. Despite the infinite number of T-t histories capable of producing the observed age and track length data, generated thermal paths are remarkably reproducible (Figure 5) and are in good agreement with independent geologic data, such as postexhumation regional subsidence histories.

6.1. North - South Transect

Samples from the north-south transect were collected from five areas along a 70-km north-south transect of the Maksyutov Complex to determine whether there was any differential movement during exhumation along the length of the complex. Modeling indicates that there was no significant difference in the timing or mechanism of late stage exhumation between the northern and southern regions of the Maksyutov Complex.

6.2. East - West Transect

The largest group of AFT samples were collected along a 5-km transect through all three units of the Maksyutov Complex at Karayanova. Modeling for these samples indicates that the three units cooled through 110°C at ~315 Ma; the similarity in thermal histories for the different units rules out major interunit movement within the Maksyutov Complex after 315 Ma. The three units of the Maksyutov Complex must have been tectonically juxtaposed after the HP event at 375 Ma that affected Unit 1 and before 315 Ma.

6.3. Hanging Wall Versus Footwall

Modeling for all samples in the Maksyutov Complex shows that they were exhumed and cooled through 110°C at ~315 Ma.

Table 1. Apatite Fission Track Results From the Maksyutov Complex, Urals

Sample Number	Sample Location and Description	Latitute, Longitude, deg.	Elevation, m	Number of Grains	ρd (x10^6) (Nd)	ρs (x10^6) (Ns)	ρi (x10^6) (Ni)	AFT Age ±1σ, Ma	P(χ^2), %	Mean Track Length ± 1σ (*N*), μm
MC29-94	Maksyutovo: unit 1 mica schist	N52°17.10', E57°46.00'	460	26	1.831 (5077)	6.499 (532)	8.576 (702)	236.2±13.8	88	12.25±0.18 (100)
MC33-94	Maksyutovo: unit 2 quartzite	N52°17.00', E57°46.00'	460	29	1.504 (4367)	6.840 (655)	8.637 (827)	210.4±12.5	85	13.08±0.17 (100)
MC87-95	Near Mikhailovka: unit 1 mica schist	N52°06', E57°46'	700	30	1.537 (4525)	7.985 (128)	8.172 (131)	261.9±32.8	100	13.30±0.12 (100)
MC21-94	Karayanova: unit 1 quartzite	N52°00.18', E57°47.18'	315	30	1.504 (4367)	1.954 (337)	2.116 (365)	242.6±18.7	100	13.71±0.13 (100)
MC99-95	Karayanova: unit 1 eclogite	N52°00.18', E57°47.38'	315	21	1.849 (5077)	4.261 (314)	5.211 (384)	263.7±20.4	100	13.39±0.20 (28)
MC178-95	Karayanova: unit 1 blueschist	N52°59.48', E57°47.18'	315	30	1.512 (4525)	2.842 (554)	2.832 (552)	264.7±16.4	100	13.99±0.13 (100)
MC65-95	Karayanova: Yumaguzinskaya graphite mica schist	N52°00.18', E57°47.15'	355	30	1.849 (5077)	4.076 (447)	4.925 (540)	260.9±16.7	99	12.78±0.16 (100)
MC126-95	Karayanova unit 2 graphite schist	N52°00.24', E57°47.17'	315	30	1.521 (4525)	1.167 (226)	1.126 (218)	274.7±26.4	100	13.15±0.10 (100)
MK115	Karayanova: unit 2 metasomatite	N52°00.01', E57°45.68'	500	30	1.831 (5077)	0.991 (94)	1.012 (96)	311.5±45.4	100	12.64±0.39 (30)
MC116-95	Antingan unit 1 blueschist	N51°53.03', E57°53.50'	460	30	1.521 (4525)	1.130 (1237)	1.183 (1295)	253.5±10.8	99	13.70±0.13 (100)
MC154-95	Shubino: unit 1 eclogite	N51°39.61', E57°55.42'	515	30	1.496 (4367)	4.181 (556)	4.384 (583)	249.0±15.2	98	13.82±0.10 (150)
MC161-95	Shubino: unit 1 eclogitic schist	N51°40.80', E57°55.69'	440	30	1.512 (4525)	8.015 (175)	8.107 (177)	260.8±28.1	100	13.44±.015 (100)
UM19A	Shubino: unit 1 eclogite	N51°39.41', E57°55.42'	515	23	1.813 (5077)	6.134 (737)	7.391 (888)	262.4±13.6	69	12.84±0.23 (84)
MC143-95	near Novopokrovka: quartzite	N51°30.48', E58°59.94'	360	30	1.525 (4525)	9.485 (123)	9.022 (117)	279.2±36.3	100	12.98±0.21 (57)
MC144-95	near Novopokrovka: quartzite	N51°30.48', E58°00.89'	360	8	1.469 (4367)	1.741 (308)	2.300 (407)	198.4±15.3	52	12.92±0.20 (55)

Abbreviations are as follows: Elevation, sample elevation; ρs, spontaneous track density (x 10^6 tracks per square centimeter); Ns, number of spontaneous tracks counted; ρi, induced track density in external detector (muscovite) (x 10^6 tracks per square centimeter); Ni, number of induced tracks counted; P(χ^2), χ^2 probability [*Galbraith*, 1981; *Green*, 1981]; ρd, induced track density in external detector adjacent to dosimetry glass (x 10^6 tracks per square centimeter); Nd, number of tracks counted in determining ρd. Age is the sample central fission track age; central age is given [*Galbraith and Laslett*, 1993] and calculated using zeta calibration method [*Hurford and Green*, 1983]. Samples were analyzed by D.F. Stockli (zeta value 356±8 for CN5).

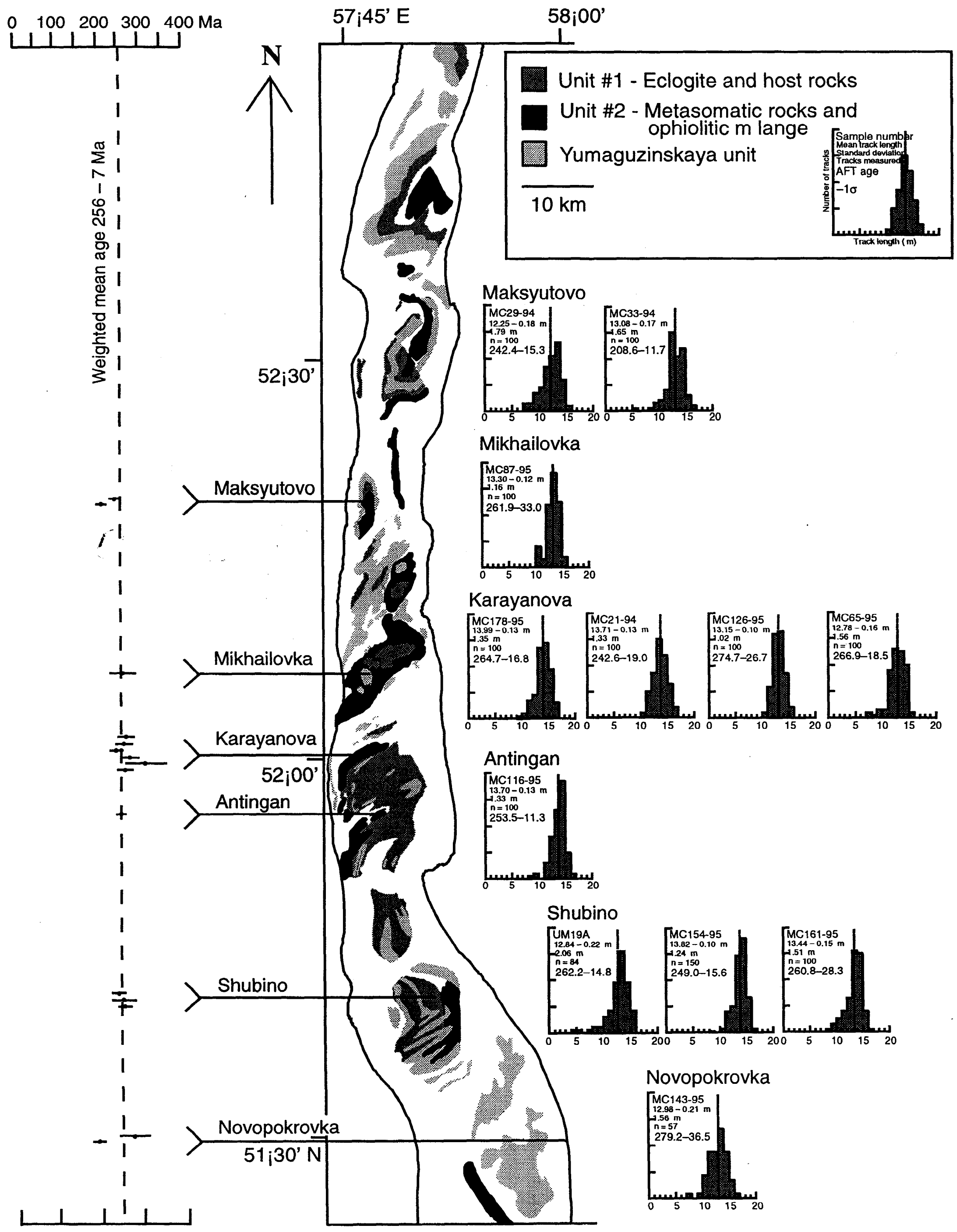

Figure 3. Detailed map of the Maksyutov Complex showing the extent of exposure throughout the complex based on Russian mapping (adapted from *Beane* [1997]). Apparent AFT ages are listed for the different sample areas; most samples intersect the weighted mean age of 256 ± 7 Ma within 1σ error. Confined track length distributions are listed for all samples with n > 80 (hanging wall sample MC-143-95 is included for comparative purposes).

Figure 6 superimposes modeled paths from Unit 1 at Shubino (MC154-95 and MC161-95) onto those of an Ordovician metasediment from the hanging wall of the MUF (MC-143-95). While modeling indicates that this metasediment sample was never heated to the extent that Maksyutov samples were, there is evidence for minor movement on the MUF until ~300 Ma after which the footwall and hanging wall have a common history.

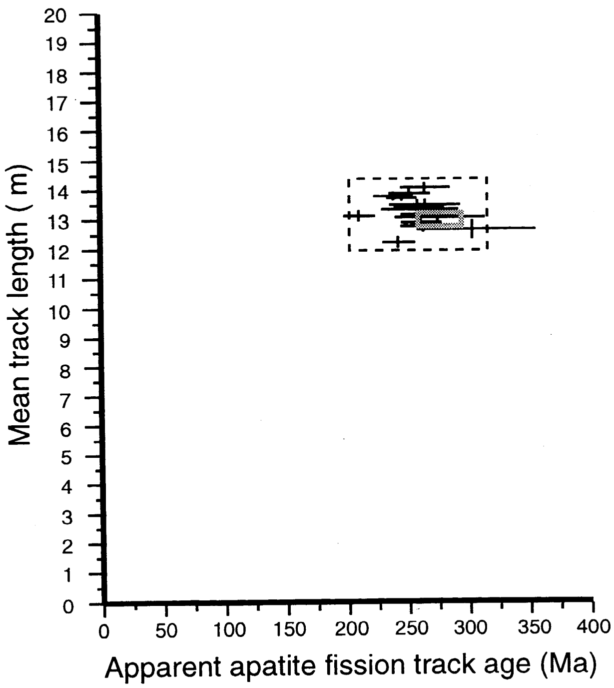

Figure 4. Plot of mean track lengths versus AFT ages for footwall samples from Maksyutov. The hanging wall sample MC-143-95 is plotted as a rectangle, showing no difference from footwall samples.

7. Thermotectonic Evolution

The fission track data and modeling constrain the following thermotectonic episodes for the low-temperature evolution of the Maksyutov Complex in the context of the overall geodynamic setting of the south Ural Mountains.

7.1. 375 to 315 Ma

After undergoing UHP metamorphism, apatite fission track and $^{40}Ar/^{39}Ar$ data suggest exhumation of the Maksyutov Complex and cooling through a temperature of 110°C between 375 and 315 Ma (Figure 7, stage 1). This cooling event roughly coincides with the onset of the Uralian collision between the East European platform and microcontinental blocks starting in the Early Devonian [*Brown et al.*, 1996]. The three units of the Maksyutov Complex must have been tectonically juxtaposed within the subduction zone sometime during this time interval.

7.2. 315 to 230 Ma

After cooling to 100 - 80°C, fission track modeling indicates minor reheating but in most cases slower monotonic cooling between ~315 and 230 Ma (Figure 7, stage 2). While modeling cannot resolve this stage in detail, reheating or the relative slowing down in cooling rate for different models are both responses to overburden; therefore we interpret this reheating event as the result of tectonic reburial of the Maksyutov Complex due to thrusting on the MUF during the main phase of Uralian convergence. This is consistent with the Maksyutov Complex forming the footwall to the MUF and being overridden by ophiolite thrust sheets [*Matte et al.*, 1993]. Modeling indicates a common history for footwall and hanging wall samples (i.e. minor to no movement on the MUF) after the late Carboniferous (300 Ma).

7.3. 230 to 180 Ma

Renewed cooling and/or continued cooling (~ 40°C) at the end of the Uralian orogeny is best interpreted as postcollisional erosional degradation of the mountain belt. It is possible that this stage represents postorogenic extensional unroofing related to the extensional reactivation of the MUF (Figure 7, stage 3) as suggested by several workers [*Matte et al.*, 1993; *Echtler and Hetzel*, 1997], but modeling cannot resolve significantly different histories for the footwall and hanging wall after ~300 Ma.

7.4. Post-180 Ma

The small temperature increase (or complete cessation of cooling) beginning ~180 Ma correlates with the end of tectonism in the Late Permian, which is followed by the erosional degradation (peneplanation) of the Urals and a marine transgression in the Jurassic [*Brown et al.*, 1996; *Seward et al.*, 1997]. Fission track data show minor but gradual reheating (~20°C), probably related to this transgression in which Jurassic and Cretaceous marine sediments were deposited on the MUF and the foreland fold-and-thrust belt (Figure 7, stage 4).

7.5. ~45 Ma to Present

Final erosional denudation of the Maksyutov Complex and exhumation to the present-day surface probably started in the Tertiary (Figure 7, stage 5). Sediments would have been shed to the foreland basin to the west. However, the exact nature of this part of the *T-t* evolution is only poorly constrained, because samples were in the total stability zone for apatite fission tracks.

8. Correlation With Other Fission Track Results From the Urals

Seward et al. [1997] collected samples for fission track dating along the 200-km west-east URSEIS seismic reflection profiling line [*Berzin et al.*, 1996; *Carbonell et al.*, 1996; *Echtler et al.*, 1996; *Knapp et al.*, 1996] north of the Maksyutov Complex (see Figure 1). Apparent AFT data range from ~180 to 210 Ma [*Seward et al.*, 1997] while zircon fission track ages from near the MUF range from 226 to 288 Ma in both the footwall and hanging wall of the fault [*Seward et al.*, 1997]. These fission track data suggest that the south central Urals have behaved as a single tectonic unit since the Early Triassic.

Combining apparent apatite and zircon age data with modeling, *Seward et al.* [1997] conclude that a regional cooling event occurred between ~280 and 210 Ma across the south Urals; a small temperature increase (~10 - 30°*C*) from

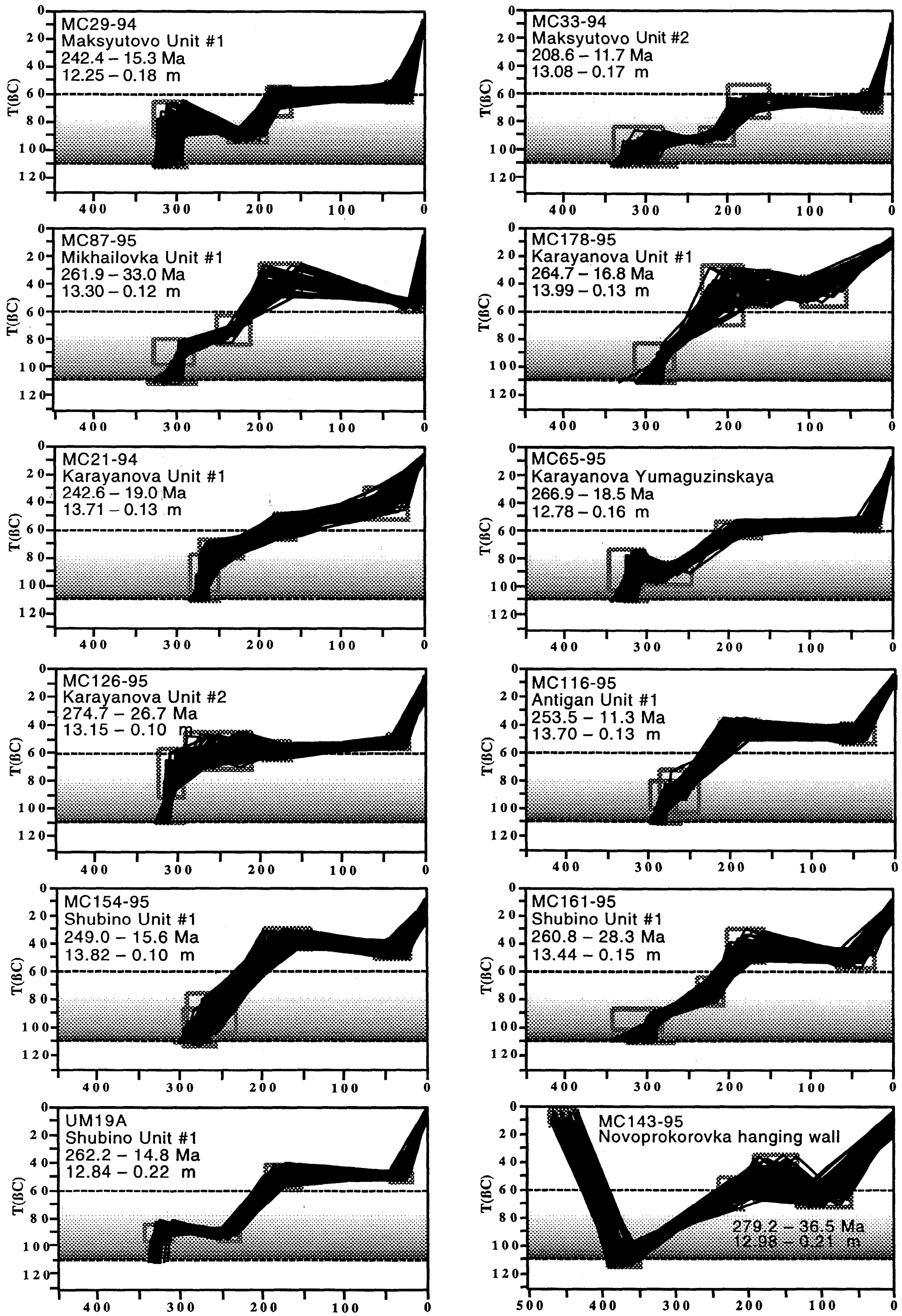

Figure 5. Modeling results for individual samples with confined track lengths $n > 80$; MC-143-95 is shown for comparison with footwall samples.

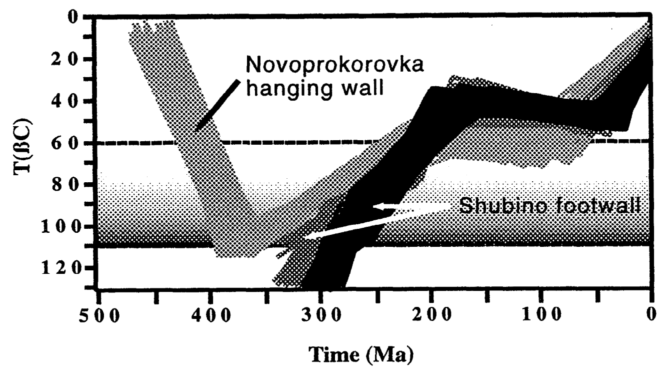

Figure 6. Modeling results for one hanging wall sample (MC-143-95) with footwall samples from nearby Shubino (MC154-95 and MC161-95) superimposed to show a probable common history after ~300 Ma.

~180 to 110 Ma is interpreted as caused by burial in the Late Jurassic and Cretaceous before final denudation starting in the Cretaceous. As described in section 7, similar events are seen in modeling from Maksyutov data that indicate regional cooling and/or gradual reheating between 300 and 230 Ma and reheating from 180 to 45 Ma.

9. Tectonic Implications of Fission Track Data

9.1. Heat Flow Data

The central axis of the Urals is characterized by anomalously low modern heat flow, ranging from ~24 to 43 mW m^{2} with an average of 35 mW m^{2} for 26 measurements in boreholes typically 1 to 3 km deep [*Kukkonen et al.*, 1997]. Periglacial climatic conditions during the last glacial period require a depth-dependent correction of +/- 5 mW m^{2} for heat flow data based on measurements in the area [*Kukkonen et al.*, 1997]. Therefore the range of present-day geothermal gradients for this region is 6° - 16°C km^{-1}, using an average conductivity value of 3.0 mW m^{-1} K^{-1}.

It is clear from the fission track samples from both this study and that of *Seward et al.* [1997] that U content in both apatite and zircon (the only common U- and Th-bearing minerals) is low, implying low radiogenic heat production. Overall, rocks exposed in the footwall of the MUF have the lowest values of heat production (from U, Th, and K concentrations) across the Urals; these mostly mafic rocks have values between 0.04 and 0.37 μW m^{3} [*Kukkonen et al.*, 1997]. Deep seismic sounding data suggest that the central Urals are characterized by abundant mafic rocks at depth, coinciding with the thick crustal root and a gravity anomaly

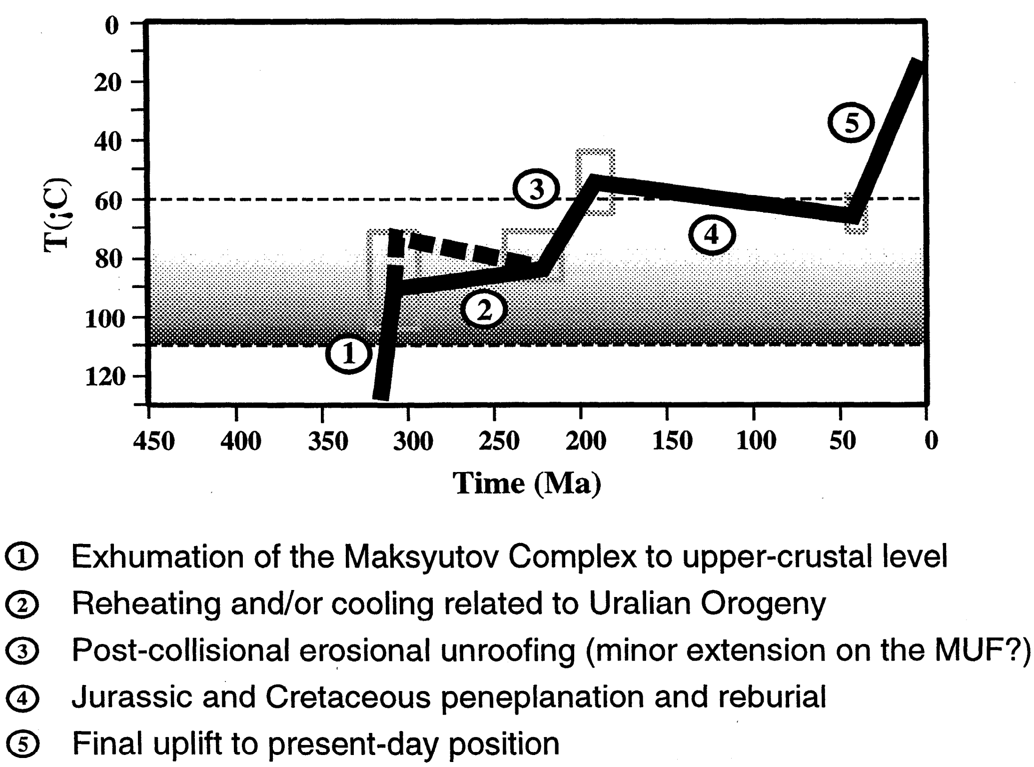

Figure 7. Summary of modeling for all AFT samples in the Maksyutov Complex showing five stages in the exhumation history since the high-grade metamorphic event. Rectangles show the error limits for each inflection point in the exhumation curve.

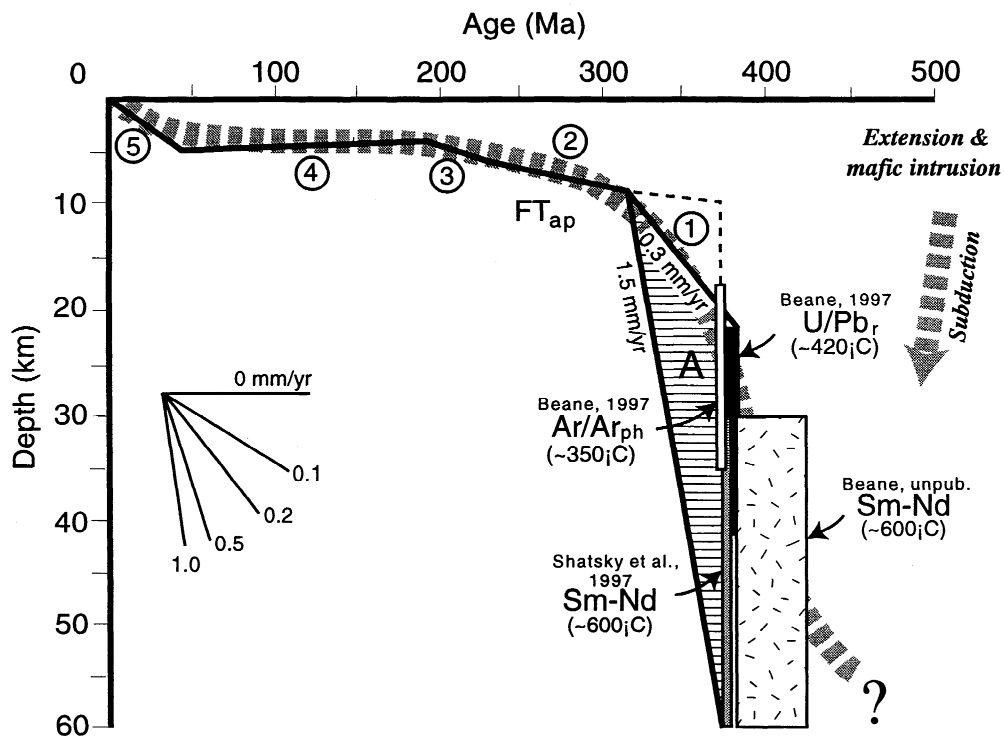

Figure 8. Depth-age path for the Maksyutov Complex. Vertical bars show the range of ages for different dating techniques based on closure temperatures for the specific radiogenic systems; the wide range of depths correspond to these closure temperatures and are based on a range of geothermal gradients from 10°C km^{-1} for current heat flow data to 20°C km^{-1} to correct for possible paleoclimatic effects [*Lachenbruch and Sass*, 1977]. Stages 1 - 5 correspond to those in Figure 7. Triangle A indicates exhumation rates from the high-grade event to cooling through 110°*C*. The dashed line shows an exhumation path allowed by higher-temperature thermochronology; fission track modeling indicates a much steeper slope for stage 1, making this path improbable.

maximum, thereby explaining, at least in part, the low heat flow [*Kukkonen et al.*, 1997]. Because this low U-Th content presumably dates at least from the Permian Uralian orogeny, we infer that heat production and hence heat flow and thermal gradients have been low at least since Permian time.

9.2. Exhumation Rate

Exhumation rates since the onset of the Uralian collision (i.e., after ~375 Ma) are best calculated using modern heat flow data [*Kukkonen et al.*, 1997]. Using the geothermal gradients calculated from heat flow data in conjunction with age data for various thermochronometry for the Maksyutov Complex, we have calculated a range of possible exhumation rates for the UHP Unit 1. Cooling to 110°*C* using the mean estimated geothermal gradient (11°C km^{-1}) implies exhumation at 0.03 mm yr^{-1} (see Figure 8). Pre-375 Ma exhumation rates are at present impossible to establish, because published high-temperature thermochronology data (Sm-Nd, ~600°*C*, 375 ± 3 Ma) overlap with published intermediate-temperature systems ($^{40}Ar/^{39}Ar$, ~350°*C*, 374 ± 2 Ma; U/Pb, ~420°*C*, 377 ± 3 Ma). However, the existence of a Devonian Sm-Nd age of 404 ± 20 Ma (R.J. Beane, unpublished data, 1997) suggests either ~30 Ma of high-temperature isothermal reequilibration from ~405 to ~375 Ma or at least relatively slow cooling. The maximum possible exhumation rate between the 404 ± 20 Ma Sm-Nd age and the 374 ± 2 Ma $^{40}Ar/^{39}Ar$ age is 2.5 mm yr^{-1} using a minimal 10°C km^{-1} geothermal gradient [*Lachenbruch and Sass*, 1977]; it is important to note that even this rate is the peak rate experienced by the Maksyutov Complex and can only have been sustained for a short time (no more than ~10 Myr). This maximum calculated exhumation rate assumes that the ~375 Ma Sm-Nd data of *Shatsky et al.* [1997] is accurate and dates the UHP event. It is more probable that the UHP event occurred earlier (i.e., >404 Ma), decreasing the exhumation rate to less than 1.0 mm yr^{-1}.

In contrast, reported exhumation rates for other UHP terranes are much higher at 5 - 25 mm yr^{-1} for the Dabie Shan [*Webb et al.*, 1999], 6 mm yr^{-1} for the Kokchetav Massif [*Ernst et al.*, 1997], and ~3 mm yr^{-1} for the Dora Maira Massif [*Hacker and Peacock*, 1995] elapsed over ~15 - 35 Myr. [*Webb et al.*, 1999]. The significantly faster published exhumation rates for other UHP terranes (the Kokchetav Massif and the Dabie Shan) explain the preservation of UHP indicator minerals such as diamond and coesite [e.g., *Dobrzhinetskaya et al.*, 1995; *Okay*, 1993; *Sobolev and Shatsky*, 1990]. *Leech and Ernst* [1998] suggested that the Maksyutov Complex underwent UHP metamorphism, on the basis of possible graphite pseudomorphs after diamond similar to those found in the Beni Bousera and Ronda peridotite massifs [e.g., *Pearson et al.*, 1989; *Davies et al.*, 1993]. Triangle A in Figure 8 indicates the range of depths and ages used for calculating exhumation rates from the high-grade event to cooling through 110°*C*; rates of 0.3 to 1.5 mm yr^{-1} were calculated using the mean geothermal gradient of 11 °C km^{-1}. Although a faster rate is possible on the basis of higher-temperature chronometers (see the dashed line in Figure 8), fission track modeling indicates a steeper slope for stage 1 and supports our slower calculated rates.

Diamond is preserved in the Kokchetav Massif under only very special conditions, chiefly as armored micro-inclusions in garnet and zircon, which acted as pressure vessels [*Sobolev and Shatsky*, 1990; *Sobolev et al.*, 1994]; moreover, a high exhumation rate did not allow the diamond-bearing rocks to reside at depth long enough to reequilibrate to graphite. Our calculated exhumation rates for the Maksyutov Complex (0.3 to 1.5 mm yr^{-1}) support the findings of *Leech and Ernst* [1998] that even coarse-grained diamond could not be preserved. Finally, because microdiamonds are only preserved as inclusions in resistant container minerals and are prevented from interacting with an aqueous fluid phase, such phases are more likely to be preserved than grains in the matrix as described in the Maksyutov carbonaceous metasediments.

10. Conclusions

The AFT data for the Maksyutov Complex describe the low-temperature evolution of Maksyutov rocks, which is consistent with the geodynamic postcollisional evolution for the south Urals. The fission track data indicate that UHP eclogites and metasediments underwent a period of exhumation between ~375 and 315 Ma; exhumation rates for this earlier stage in the evolution of the complex range from 0.3 to 1.5 mm yr^{-1}, using mean current heat flow data. These exhumation rates are slow compared to other UHP terranes and support the earlier finding of *Leech and Ernst* [1998], based on graphite pseudomorphs after diamond, that relict UHP coesite or diamond should not have been preserved in the Maksyutov Complex. Considering that slow exhumation rates remove most evidence for UHP metamorphism, perhaps it is more widespread globally than has been appreciated.

This period of exhumation was followed by a slowed cooling rate or reheating perhaps due to thrusting along the MUF and subsequent tectonic reburial of the Maksyutov Complex while remaining within the PAZ. At the end of the Uralian orogeny (~230 Ma), the rocks underwent an episode of cooling (~40°*C*) interpreted as erosional degradation of the orogen. This stage may indicate possible minor postorogenic extension and reactivation of the MUF as a normal fault, but modeling cannot resolve significantly different histories between the footwall and hanging wall after ~300 Ma. This cooling episode was followed by an extended period of time during which the samples resided at ~60°*C* which is consistent with a regional marine transgression reported by *Seward et al.* [1997] for fission track samples along the URSEIS seismic profile. This marine transgression buried the area in the Jurassic and Cretaceous starting at ~180 Ma and was followed by a regional peneplanation and final exhumation to the surface at ~45 Ma.

Apatite fission track results suggest that interunit thrusting was complete before ~315 Ma. Because $^{40}Ar/^{39}Ar$ cooling ages are different for the three units of the Maksyutov Complex, they must have been tectonically juxtaposed between the youngest $^{40}Ar/^{39}Ar$ ages for Unit 2 at ~335 Ma [*Beane*, 1997] and 315 Ma. The north-south transect through Maksyutov indicates that exhumation was concurrent throughout the complex and that there was no differential movement between the north and south regions. Comparing AFT modeling results for Maksyutov samples and an Ordovician metasediment from the hanging wall of the MUF, it is clear that movement on the MUF was minor and that the footwall and hanging wall had a common cooling history after about the late Carboniferous (300 Ma).

Modeling results indicate cooling at the end of collision in the Uralian orogeny; the MUF was probably reactivated as an extensional structure until ~300 Ma. A combination of thrusting to the west along a structure like the Zuratkul fault (see Figure 2) and early normal faulting on the MUF probably exhumed the Maksyutov Complex to upper crustal levels; this corresponds to exhumation mechanisms for other UHP terranes [*Ernst et al.*, 1997] and evidence from reflection seismic profiles [*Echtler and Hetzel*, 1997; *Hetzel et al.*, 1998]. The fission track data do not show that there was major, late extension on the MUF, and because the Urals are characterized by very low heat flow, this may explain in part the lack of large-scale postorogenic collapse. These new data on the evolution of the Maksyutov Complex allow age constraints on major events during the formation of the south Ural Mountains that were missing in previous tectonic evolution models [e.g., *Matte et al.*, 1993; *Matte*, 1995; *Chemenda et al.*, 1997]. Understanding the entire *P-T-t* evolution of a metamorphic complex employing high- to low-temperature chronometers and using these methods to constrain movement on major structures such as the MUF will help greatly in the overall understanding of exhumation mechanisms for the Maksyutov Complex and other UHP terranes.

Acknowledgments. Thanks to Trevor Dumitru, Jim Knapp, Diane Seward, and one anonymous reviewer for very helpful and thorough reviews; to Simon Klemperer for helpful input and discussion; and to Rachel Beane for mineral separates. Partial funding for this research in the Maksyutov Complex was derived from a research grant to Mary L. Leech (6075-97) from the Geological Society of America and McGee and Shell Fund grants from Stanford University (Mary L. Leech).

References

Beane, R.J., Petrologic evolution and geochronologic constraints for high-pressure metamorphism in the Maksyutov Complex, south Ural Mountains, Ph.D. dissertation, 133 pp., Stanford Univ., Stanford, Calif., 1997.

Beane, R.J., J.G. Liou, R.G. Coleman, and M.L. Leech, Mineral assemblages and retrograde P-T path for high- to ultrahigh-pressure metamorphism in the lower unit of the Maksyutov Complex, Southern Ural Mountains, Russia, *Island Arc*, *4*, 254-266, 1995.

Beane, R.J., J.G. Liou, and J.N. Connelly, Evidence for Devonian eclogite-facies metamorphism in the Maksyutov Complex, Southern Ural Mountains, Russia, *Geol. Soc. Am. Abstr. Programs, 28*, 170, 1996.

Berzin, R., O. Oncken, J.H. Knapp, A. Perez-Estaún, T. Hismatulin, N. Yunosov, and A.

Lipilin, Orogenic evolution of the Ural Mountains: Results from an integrated seismic experiment, *Science*, *274*, 220-221, 1996.

Bohlen, S.R., and A.L. Boettcher, The quartz ↔ coesite transformation: A precise determination and the effects of other components, *J. Geophys. Res.*, *87*, 7073-7078, 1982.

Brown, D., and P. Spadea, Processes of forearc and accretionary complex formation during arc-continent collision in the southern Ural Mountains, *Geology*, *27*, 649-652, 1999.

Brown, D., V. Puchkov, J. Alvarez-Marron, and A. Perez-Estaun, The structural architecture of the footwall to the Main Uralian Fault, southern Urals, *Earth Sci. Rev.*, *40*, 125-147, 1996.

Brown, D., C. Juhlin, J. Alvarez-Marron, A. Pérez-Estaún, and A. Oslianski, Crustal-scale structure and evolution of an arc-continent collision zone in the southern Urals, Russia, *Tectonics*, *17*, 158-171, 1998.

Carbonell, R., A. Perez-Estaún, J. Gallart, J. Diaz, S. Kashubin, J. Mechie, R. Stadtlander, A. Schulze, J. H. Knapp, and A. Morozov, Crustal root beneath the Urals: Wide-angle seismic evidence, *Science*, *274*, 222-224, 1996.

Chemenda, A., P. Matte, and V. Sokolov, A model of Palaeozoic obduction and exhumation of high-pressure/low-temperature rocks in the southern Urals, *Tectonophysics*, *276*, 217-227, 1997.

Chesnokov, B.V., and V.A. Popov, Increasing volume of quartz grains in eclogites of the South Urals, *Dokl. Akad. Nauk SSSR*, *162*, 176-178, 1965.

Coleman, R.G., J.G. Liou, R. Zhang, N. Dobretsov, V. Shatsky, and V. Lennykh, Tectonic setting of the UHPM Maksyutov Complex, Ural Mountains, Russia, *Eos Trans. AGU*, *74*, (43), Fall Meet. Suppl., F547, 1993.

Corrigan, J.D., Inversion of apatite fission track data for thermal history information, *J. Geophys. Res.*, *96*, 10,347-10,360, 1991.

Corrigan, J.D., Annealing models under the microscope, *On Track*, *2*, 9-11, 1992.

Crowley, K. D., M. Cameron, and R.L. Schaefer, Experimental studies of annealing of etched fission tracks in fluorapatite, *Geochim. Cosmochim. Acta*, *55*, 1449-1465, 1991.

Davies, G. R., P.H. Nixon, D.G, Pearson, and M. Obata, Tectonic implications of graphitized diamonds from the Ronda peridotite massif, southern Spain, *Geology*, *21*, 471-474, 1993.

Dewey, J.F., Extensional collapse of orogens, *Tectonics*, *7*, 1123-1139, 1988.

Diaconescu, C.C., J.H. Knapp, L.D. Brown, D.N. Steer, and M. Stiller, Precambrian Moho offset and tectonic stability of the East European platform from the URSEIS deep seismic profile, *Geology*, *26*, 211-214, 1998.

Dobretsov, N.L., and L.V. Dobretsova, New mineralogic data on the Maksyutovo eclogite-glaucophane schist complex, southern Urals, *Dokl. Akad. Nauk SSSR*, *300*, 111-116, 1988.

Dobretsov, N.L., V.S. Shatsky, R.G. Coleman, V.I. Lennykh, P.M. Valizer, J.G. Liou, R. Zhang, and R.J. Beane, Tectonic setting and petrology of ultrahigh-pressure metamorphic rocks in the Maksutov complex, Ural Mountains, Russia, *Int. Geol. Rev.*, *38*, 136-160, 1996.

Dobrzhinetskaya, L. F., E.A. Eide, R.B. Larsen, B.A. Sturt, R.G. Tronnes, D.C. Smith, W.R. Taylor, and R.V. Posukhova, Microdiamond in high-grade metamorphic rocks of the Western Gneiss region, Norway, *Geology*, *23*, 597-600, 1995.

Dodson, M.H., Closure temperature in cooling geochronologic and petrologic systems, *Contrib. Mineral. Petrol.*, *40*, 259-274, 1973.

Dumitru, T.A., A new computer-automated microscope stage system for fission track analysis, *Nuclear Tracks and Radiation Measurements*, *21*, 575-580, 1993.

Dumitru, T.A., Fission-track geochronology, in *Geophys. Monogr. Ser.*, edited by J.S. Noller, J.M. Sowers, and W.R. Lettis, AGU, Washington, D.C., in press, 2000.

Echtler, H.P., and R. Hetzel, Main Uralian Thrust and Main Uralian Normal Fault: Non-extensional Palaeozoic high-P rock exhumation, oblique collision, and normal faulting in the southern Urals, *Terra Nova*, *9*, 158-162, 1997.

Echtler, H.P., et al., Preserved collisional crustal structure of the Southern Urals revealed by vibroseis profiling, *Science*, *274*, 224-226, 1996.

Edwards, R.L., and G.J. Wasserburg, The age and emplacement of obducted oceanic crust in the Urals from Sm-Nd and Rb-Sr systematics, *Earth Planet. Sci. Lett.*, *72*, 389-404, 1985.

Ernst, W.G., S. Maruyama, and S. Wallis, Buoyancy-driven, rapid exhumation of ultrahigh-pressure metamorphosed continental crust, *Proc. Natl. Acad. Sci. U.S.A.*, *94*, 9532-9537, 1997.

Fitzgerald, P.G., and A.J.W. Gleadow, New approaches in fission track geochronology as a tectonic tool: Examples from the Transantarctic Mountains, *Nucl. Tracks*, *17*, 351-357, 1990.

Fleischer, R.L., P.B. Price, and R.M. Walker, *Nuclear Tracks in Solids*, Univ. of Calif. Press, Berkeley, 1975.

Galbraith, R. F., On statistical models for fission track counts, *Math. Geol.*, *13*, 471-478, 1981.

Galbraith, R.F., and G.M. Laslett, Statistical methods for mixed fission track ages, *Nucl. Tracks Rad. Meas.*, *21*, 459-470, 1993.

Gallagher, K., Evolving temperature histories from apatite fission-track data, *Earth Planet. Sci. Lett.*, *136*, 421-435, 1995.

Gleadow, A.J.W., I.R. Duddy, P.F. Green, and K.A. Hegarty, Fission track lengths in the apatite annealing zone and the interpretation of mixed ages, *Earth Planet. Sci. Lett.*, *78*, 245-254, 1986a.

Gleadow, A.J.W., I.R. Duddy, P.F. Green, and J.F. Lovering, Confined fission track lengths in apatite: A diagnostic tool for thermal history analysis, *Contrib. Mineral. Petrol.*, *94*, 405-415, 1986b.

Green, P.F., A new look at statistics in fission track dating, *Nucl. Tracks Rad. Meas.*, *5*, 77-86, 1981.

Green, P.F., I.R. Duddy, A.J.W. Gleadow, and J.F. Lovering, Apatite fission-track analysis as a paleotemperature indicator for hydrocarbon exploration, in *Thermal History of Sedimentary Basins: Methods and Case Histories*, edited by N.D. Naeser and T.H. McCulloh, pp. 181-195, Springer-Verlag, New York, 1989a.

Green, P.F., I.R. Duddy, G.M. Laslett, K.A. Hegarty, A.J.W. Gleadow, and J.F. Lovering, Thermal annealing of fission tracks in apatite, 4, Quantitative modelling techniques and extension to geological timescales, *Chem. Geol.*, *79*, 155-182, 1989b.

Hacker, B.R., and S.M. Peacock, Creation, preservation, and exhumation of UHPM rocks, in *Ultrahigh Pressure Metamorphism*, edited by R.G. Coleman and X. Wang, pp. 159-181, Cambridge Univ. Press, New York, 1995.

Hetzel, R., H.P. Echtler, W. Seifert, B.A. Schulte, and K.S. Ivanov, Subduction- and exhumation-related fabrics in the Paleozoic high-pressure—low-temperature Maksyutov Complex, Antingan area, southern Urals, Russia, *GSA Bull.*, *110*, 916-930, 1998.

Holland, T.J.B., The reaction albite = jadeite+quartz determined experimentally in the range 600-1200 degrees C, *Am. Mineral.*, *65*, 129-134, 1980.

Hurford, A.J., and P.F. Green, The zeta age calibration of fission-track dating, *Isotope Geosci.*, *1*, 285-317, 1983.

Knapp, J.H., et al., Lithosphere-scale seismic image of the Southern Urals from explosion-source reflection profiling, *Science*, *274*, 226-228, 1996.

Knapp, J.H., C.C. Diaconescu, M.A. Bader, V.B. Sokolov, S.N. Kashubin, and A.V. Rybalka, Seismic reflection fabrics of continental collision and post-orogenic extension in the Middle Urals, central Russia, *Tectonophysics*, *288*, 115-126, 1998.

Kukkonen, I.T., I.V. Golovanova, Y.V. Khachay, V.S. Drushinin, A.M. Kosarev, and V.A. Schapov, Low geothermal heat flow of the Urals fold belt: Implication of low heat production, fluid circulation or palaeoclimate?, *Tectonophysics*, *162*, 63-85, 1997.

Lachenbruch, A.H., and J.H. Sass, Heat flow in the United States and the thermal regime of the crust, in *The Earth's Crust: Its Nature and Physical Properties, Geophys. Monogr. Ser.*, vol. 20, edited by J.G. Heacock, pp. 626-675, AGU, Washington, D.C., 1977.

Laslett, G.M., W.S. Kendall, A.J.W. Gleadow, I.R. Duddy, I. R, Bias in measurement of fission-track length distributions, *Nucl. Tracks and Rad. Meas.*, *6*, 79-85, 1982.

Laslett, G.M., P.F. Green, I.R. Duddy, and A.J.W. Gleadow, Thermal annealing of fission tracks in apatite, 2, A quantitative analysis, *Chem. Geol.*, *65*, 1-13, 1987.

Leech, M.L., and W.G. Ernst, Graphite pseudomorphs after diamond?: A carbon isotope and spectroscopic study of graphite cuboids from the Maksyutov Complex, south Ural Mountains, Russia, *Geochim. Cosmochim. Acta*, *62*, 2143-2154, 1998.

Lennykh, V.I., P.M. Valizer, R.J. Beane, M.L. Leech, and W.G. Ernst, Petrotectonic evolution of the Maksyutov Complex, south Urals, Russia: Implications for ultrahigh-pressure metamorphism, *Int. Geol. Rev.*, *37*, 584-600, 1995.

Matte, P.H., Southern Uralides and Variscides: Comparison of their anatomies and evolutions, *Geol. Mijnbouw*, *74*, 151-166, 1995.

Matte, P., H. Maluski, R. Caby, A. Nicholas, P. Kepezhinkskas, and S. Sobolev, Geodynamic model and $^{39}Ar/^{40}Ar$ dating for the generation and emplacement of the high pressure metamorphic rocks in SW Urals, *C. R. Acad. Sci., Ser. II*, *317*, 1667-1674, 1993.

Mezger, K., G.N. Hanson, and S.R. Bohlen, High-precision U-Pb ages of metamorphic rutile:

Application to the cooling history of high-grade terranes, *Earth Planet. Sci. Lett.*, *96*, 106-118, 1989.

Mezger, K., E.J. Essene, and A.N. Halliday, Closure temperatures of the Sm-Nd system in metamorphic garnets, *Earth Planet. Sci. Lett.*, *113*, 397-409, 1992.

Naeser, C.W., Fission track dating and geological annealing of fission tracks, in *Lectures in Isotope Geology,* edited by E. Jäger and J.C. Hunziker, pp. 154-169, Springer-Verlag, New York, 1979.

Naeser, C.W., The fading of fission tracks in the geologic environment: Data from deep drillholes, *Nucl. Tracks, 5*, 248-250, 1981.

Okay, A.I., Petrology of a diamond and coesite-bearing metamorphic terrain: Dabie Shan, China, *Eur. J. Mineral.*, *5*, 659-675, 1993.

Pearson, D.G., G.R. Davies, and P.H. Nixon, Graphitized diamonds from a peridotite massif in Morocco and implications for anomalous diamond occurrences, *Nature, 338*, 60-62, 1989.

Powell, R., Regression diagnostics and robust regression in geothermometer/geobarometer calibration: The garnet-clinopyroxene geothermometer revisited, *J. Metamorph. Geol.*, *3*, 231-243, 1985.

Puchkov, V.N., Paleo-oceanic structures of the Ural Mountains, *Geotecktonika*, *3*, 18-33, 1993.

Puchkov, V.N., Structure and geodynamics of the Uralian orogen, in *Orogeny Through Time,* edited by J.-P. Burg and M. Ford, *Geol. Soc. Spec. Publ., 121*, 201-236, 1997.

Purdy, J.W., and E. Jager, K-Ar ages on rock-forming minerals from the central alps, *Mem. Ist. Geol. Mineral. Univ. Padova*, *30*, 1-31, 1976.

Savelieva, G.N., A.Y. Sharaskin, A.A. Saveliev, P. Spadea, and L. Gaggero, Ophiolites of the southern Uralides adjacent to the East European continental margin, *Tectonophysics, 276*, 117-137, 1997.

Seward, D., A. Perez-Estaun, and V. Puchkov, Preliminary fission-track results from the southern Urals: Sterlitamak to Magnitogorsk, *Tectonophysics*, *276*, 281-290, 1997.

Shatsky, V.S., E. Jagoutz, and O.A. Koz'menko, Sm-Nd dating of the high-pressure metamorphism of the Maksyutov Complex, southern Urals, *Dokl. Akad. Sci. USSR, Earth Sci. Ser., Engl. Transl.*, *353*, 285-288, 1997.

Sobolev, N.V., and V.S. Shatsky, Diamond inclusions in garnets from metamorphic rocks, *Nature*, *343*, 742-746, 1990.

Sobolev, N.V., V.S. Shatsky, M.A. Vavilov, and S.V. Goryainov, Zircon from ultra high pressure metamorphic rocks of folded regions as a unique container of inclusions of diamond, coesite and coexisting minerals, *Dokl. Akad. Nauk, 334*, 488-492, 1994.

Tagami, T., R.F. Galbraith, R. Yamada, and G.M. Laslett, Revised annealing kinetics of fission tracks in zircon and geological implications, in *Advances in Fission-Track Geochronology*, edited by P. Van den Haute and F. Corte, pp. 99-112, Kluwer Acad., Norwell, Mass., 1998.

Webb, L.E., B.R. Hacker, L. Ratschbacher, M. McWilliams, and S. Dong, Thermochronologic constraints on deformation and cooling history of high- and ultrahigh-pressure rocks in the Qinling-Dabie orogen, eastern China, *Tectonics, 18*, 621-638, 1999.

Zakharov, O.A., and V.N. Puchkov, On the tectonic nature of the Maksyutov Complex of the Ural-Tau zone, report, 28 pp., Ufimian Sci. Cent., Russ. Acad. of Sci., Ufa, Russia, 1994.

Zalduegui, J.F.S., U. Scharer, J.I.G. Ibarguchi, and J. Girardeau, Origin and evolution of the Paleozoic Cabo Ortegal ultramafic-mafic complex (NW Spain): U-Pb, Rb-Sr and Pb-Pb isotope data, *Chem. Geol.*, *129*, 281-304, 1996.

Zonenshain, L.P., V.G. Korinevsky, V.G. Kazmin, D.M. Pecherskiy, V.V. Khain, and V.V. Matveyenkov, Plate tectonic model of the South Urals development, *Tectonophysics*, *109*, 95-135, 1984.

Zonenshain, L.P., M.I. Kuzmin, and L.M. Natapov, *Geology of the USSR: A Plate-Tectonic Synthesis*, *Geodyn. Ser.*, vol. 21, edited by L.P. Zonenshain et al., 242 pp., AGU, Washington, D.C., 1990.

M.L. Leech, Geology Department, Royal Holloway, University of London, Egham, TW20 0EX, England, U.K. (m.leech@gl.rhbnc.ac.uk)

D.F. Stockli, Geological and Planetary Sciences, California Institute of Technology, Pasadena, CA 91125. (stockli@gps.caltech.edu)

(Received December 2, 1998;
revised August 12, 1999;
accepted August 12, 1999.)